

# Microstructure and Mechanical Properties of Ti-4Al-1.5Mn Resistance Spot Welding Joints

JIANG Jian<sup>1</sup>, QI Lichun<sup>2</sup>, ZHANG Mingjie<sup>2</sup>, CHEN Wenhua<sup>1</sup>, SHEN Yifu<sup>1\*</sup>

1. College of Materials Science and Technology, Nanjing University of Aeronautics and Astronautics, Nanjing 211106, P.R. China;

2. Institute of Titanium Alloy, Beijing Institute of Aeronautical Materials, Beijing 100095, P.R. China

(Received 23 November 2020; revised 5 March 2021; accepted 30 May 2021)

**Abstract:** Ti-4Al-1.5Mn dual phase titanium alloy sheet was spot welded by pneumatic resistance spot welder. The effects of different welding parameters on shear load and nugget diameter were studied. The results show that the maximum shear load of solder joint increases first and then decreases with the increase of electrode pressure and welding current, while the nugget diameter increases with the increase of electrode pressure and welding current. Electrode pressure of 0.20 MPa and welding current of 46 A are the optimal process parameters, under which the maximum shear load of solder joint reaches 8.80 kN. The microstructure of nugget zone is coarse acicular martensite, and the solder joints fail in a mixed mode of intergranular brittle-ductile fracture.

**Key words:** titanium alloy; resistance spot welding; shear load; microstructure

**CLC number:** TG146; TG668

**Document code:** A

**Article ID:** 1005-1120(2021)05-0893-08

## 0 Introduction

Titanium and titanium alloys are widely used in aerospace, chemical, medical and other civil and military industries because of their excellent characteristics in specific strength, corrosion resistance, creep and fatigue properties, biocompatibility and so on. They can effectively meet the urgent demand for high-performance structural materials in industrial applications, such as aerospace, automotive, medical engineering<sup>[1-6]</sup>.

At present, welding and joining of titanium alloys mainly includes laser fusion brazing<sup>[7]</sup>, friction stir welding<sup>[8]</sup>, diffusion welding<sup>[9]</sup>, electron beam welding<sup>[10]</sup>, ultrasonic welding<sup>[11]</sup>, and resistance spot welding<sup>[12]</sup>. Resistance spot welding has the characteristics of high degree of automation, simple operation, low cost, good environmental applicability, and high welding energy density and high efficiency<sup>[13-14]</sup>. Therefore, the welding product has in-

finitesimal distortion and small heat affected zone, so it is widely used in welding of metal<sup>[15-16]</sup>. In resistance spot welding process, the overlapping work is positioned between the water-cooled electrodes, then the heat is generated by using a large electrical current for a short period of time. There are three stages in making spot weld. First, the electrodes are attached to the metal and pressure is applied before the current is switched on. Second, the current is turned on instantaneously. This is followed by the third stage, or hold time in which the current is turned off but the pressure continues. During the hold time, the electrodes forges the metal as it cools. The weld is formed via solidification due to cooling through the electrodes<sup>[17-18]</sup>.

During the electric current flow, due to the resistance opposed by an electric current, contact region between electrode and the material and connecting elements is subject to strong localized heating. The weld quality depends on the microstructure

\*Corresponding author, E-mail address: yifushen@nuaa.edu.cn.

**How to cite this article:** JIANG Jian, QI Lichun, ZHANG Mingjie, et al. Microstructure and mechanical properties of Ti-4Al-1.5Mn resistance spot welding joints[J]. Transactions of Nanjing University of Aeronautics and Astronautics, 2021, 38(5): 893-900.

<http://dx.doi.org/10.16356/j.1005-1120.2021.05.016>

of the nugget which is affected by heat process and cooling rate<sup>[19-21]</sup>. Feng et al.<sup>[22]</sup> carried out the fatigue property research of TA1 pure titanium spot welding joints, and analyzed the fracture mechanism of resistance spot welding joints. Jiang et al.<sup>[23]</sup> studied and analyzed the microstructure and properties of pure titanium/magnesium alloy dissimilar material resistance spot welding joints, and obtained the resistance spot welding joints with excellent performance. However, resistance spot welding of titanium alloy is mainly focused on thin plates, and there are few reports about the resistance spot welding of 2 mm thickness titanium alloy sheet.

Therefore, in this paper, resistance spot welding is used to weld 2 mm thick Ti-4Al-1.5Mn plate. The effect of resistance spot welding parameters on mechanical properties and nugget diameter is investigated. The microstructure of nugget zone and fracture morphology of solder joints are analyzed.

## 1 Materials and Methods

Ti-4Al-1.5Mn plate with dimensions of 100 mm × 10 mm × 2.0 mm is selected as the base metal, and its chemical composition is shown in Table 1. The lap length of resistance spot welding sample is 30 mm, and the shape and the size of the sample are shown in Fig. 1. The equipment adopted in this study is pneumatic resistance spot welding machine (Model: medium frequency spot welding machine DZN-200 kW). The welding discharge time is 10 ms, the electrode diameter is 4.0 mm, and the electrodes on both sides are conical CuZrCr electrodes with the end diameter of 4 mm. Before welding, the oxide and oil stain on the surface of the sample were polished with abrasive paper, and the plates were degreased with anhydrous ethanol. During welding, the lap length was kept unchanged, and the resistance spot welding process parameters are shown in Table 2. After resistance spot welding, the shear resistance test was carried out by SANS CMT-5105 electronic universal tensile testing machine according to GB/2651—2008 standard at room temperature, and the average value was obtained by testing sample at the same parameters for

three times. The cross-section microhardness of resistance spot welding joint was tested and analyzed by HXS-1000A microhardness tester. The load was 200g, and the load was maintained for 15 s before unloading. The average of three samples were measured to improve the accuracy of microhardness value. The metallographic samples were taken along the diameter direction of the solder joints, and the optical microscopy analysis of the samples was carried out by using the orca binocular XTL-2600 microscope. The microstructure of Ti-4Al-1.5Mn solder joints and fracture surface were detected with a Hitachi S-4800 field emission scanning electron microscopy (FESEM).

**Table 1 Chemical compositions of Ti-4Al-1.5Mn alloy substrate** %

| Element        | H    | N    | C     | Si   | Fe   | Mn   | B    | Al   | Ti   |
|----------------|------|------|-------|------|------|------|------|------|------|
| Weight percent | 0.06 | 0.15 | 0.012 | 0.05 | 0.08 | 1.43 | 0.22 | 4.09 | Bal. |

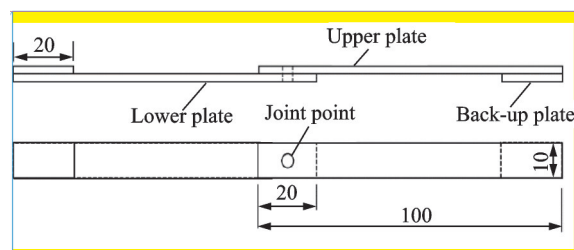


Fig.1 Schematic diagram of resistance spot welding sample

**Table 2 Resistance spot welding process parameters**

| Welding time/ms | Welding current/<br>A | Electrode pressure /<br>MPa |
|-----------------|-----------------------|-----------------------------|
| 10              | 33—65                 | 0.10—0.25                   |

## 2 Results and Discussion

### 2.1 Influence of resistance spot welding parameters on spot welding properties

#### 2.1.1 Electrode pressure

Under the condition of welding current of 52 A and welding time of 10 ms, the influence of electrode pressure on shear load and nugget diameter was revealed by adjusting the electrode pressure during spot welding. As shown in Fig.2, when the elec-

trode pressure increases from 0.10 MPa to 0.20 MPa, the shear load of resistance spot welding joints increases gradually, reaching the maximum value of 8.60 kN. When the electrode pressure continues to increase, the shear load of the resistance spot welding joints decreases gradually. The variation of nugget diameter with electrode pressure is similar to that of shear load, and it also increases first and then decreases. When the electrode pressure is low, the surface of the resistance spot welding plate is rugged, so the contact resistance between the test plates is high. According to Joule's law  $Q = I^2RT$ , the higher the contact resistance, the more heat will be produced during spot welding, resulting in spatter, and it can affect the mechanical properties of the solder joints. When the electrode pressure gradually increases, the point contact between the upper and the lower plates decreases and the surface contact increases, which results in a decrease in contact resistance. While heat input decreases, little or even no spatter occurs, and the nugget diameter also increases, which is conducive to obtain high shear load of the spot welding joints. When the electrode pressure is higher than 0.20 MPa, the Ti-4Al-1.5Mn plates are in surface contact. At this time, the heat input decreases and the heat dissipation area increases, which leads to the decrease of the shear load of the solder joints, the further decrease of the nugget diameter, and even the lack of penetration.

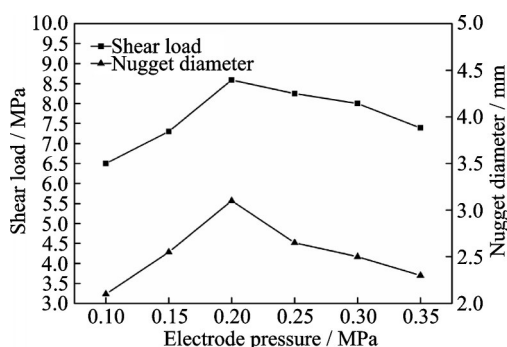


Fig.2 Effects of electrode pressure on shear load and nugget diameter of solder joints

### 2.1.2 Welding current

Under the condition of electrode pressure of

0.20 MPa and welding time of 10 ms, the influence of welding current on shear load and nugget size was analyzed by varying welding current. The change tendency of shear load of the solder joints is similar to that in Fig.2, which shows the trend of first increasing and then decreasing. With the increase of welding current, the nugget diameter of solder joints continues to increase. As shown in Fig.3, when the welding current is in the range of 33–46 A, the shear load of the solder joints increases from 6.96 kN to 8.80 kN with the increase of welding current. When the welding current exceeds 46 A, the shear load of solder joints decreases with the increase of welding current. Therefore, when the welding current is 46 A, the maximum shear load of solder joints reaches 8.80 kN. According to Joule's law  $Q = I^2RT$ , it can be found that the welding current is directly related to the heat input in spot welding process. When the heat input is low due to small welding current, the Ti-4Al-1.5Mn plate is not fully melted during the welding process, resulting in the smaller nugget diameter and the lower shear strength of the solder joints. When the welding current reaches 46 A, the metal in nugget zone is fully melted and has good metallurgical bonding. The shear load is high due to the increased diameter of nugget. While the welding current further increases, the resistance between the two electrodes becomes greater, which leads to excessive heat input, serious melting of titanium alloy, and a large number of spatter and other defects are produced at the solder joints. Finally, it greatly reduces the shear load and reliability of the solder joints.

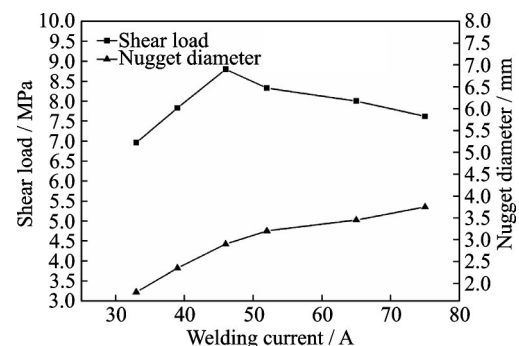
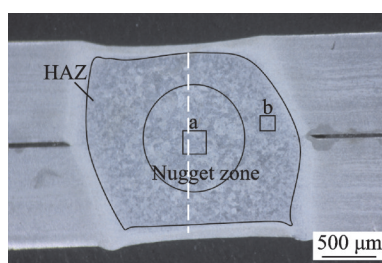


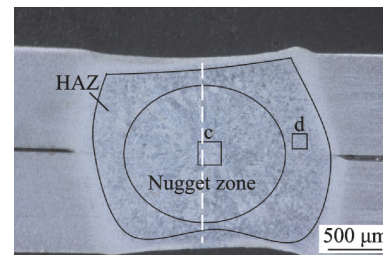
Fig.3 Effects of welding current on shear load and nugget diameter of solder joints

## 2.2 Microstructure and microhardness analysis of solder joints

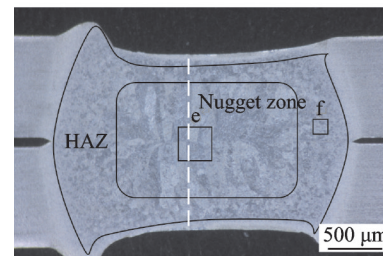
Fig.4 shows the optical morphology of resistance spot welding joints of Ti-4Al-1.5Mn titanium alloy, which is mainly composed of nugget zone (NZ) and heat affected zone (HAZ). The nugget zone has a typical as-cast structure.  $\beta$  columnar crystal is epitaxially grown by intergrowth crystallization on the basis of semi-melted grains of base metal. Moreover, due to the accumulation of heat in the weld zone, it is difficult for the heat transfer of the alloy. Under the effect of welding heat, the grain of nugget zone is very coarse, leading to the coarseness of  $\beta$ -columnar crystal. During the cooling process at the center of resistance spot welding joints,  $\alpha'$  acicular martensite transformation will occur along with the nucleation and growth of  $\beta$  columnar crystal. Fig.4 shows the cross-sectional morphology of solder joints at electrode pressures of 0.15, 0.20 and 0.25 MPa, respectively. When the electrode pressure is low, the gap between the upper and the lower plates is large. The heat transfer in the welding process can not only pass through the heat conduction of the titanium alloy plate, but also take part of the heat by the heat radiation of the air in the gap, so the grain in the nugget zone is fine. However, when the electrode pressure is too high, i. e. 0.25 MPa, the material extrusion occurs seriously, and owing to the serious accumulation of heat in the nugget zone, the grains in the nugget zone are abnormally coarse, it is harmful to the mechanical properties of the solder joints.



(a) Macrostructure of solder joint welded at  $p=0.15$  MPa



(b) Macrostructure of solder joint welded at  $p=0.20$  MPa



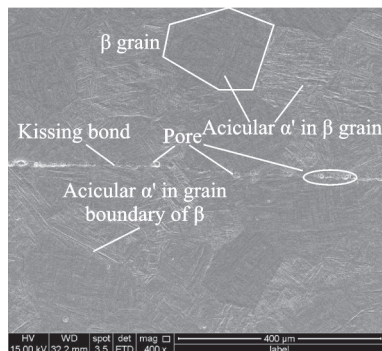
(c) Macrostructure of solder joint welded at  $p=0.25$  MPa

Fig.4 Cross section morphologies of solder joints at different electrode pressures

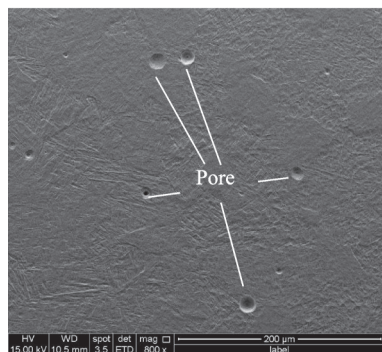
As shown in Fig.5, the microstructure of resistance spot welding joints is mainly composed of coarse needle-shaped martensite and it is distributed in a certain orientation. The growth of  $\beta$  grains is coarse due to the high temperature of the nugget zone of solder joints. During the process of  $\beta \rightarrow \alpha'$  phase transition,  $\alpha'$  phase first forms nucleus at the boundary of  $\beta$  phase and grows into the crystal. At the same time, owing to the large amount of heat input and poor thermal conductivity of titanium alloy, the cooling speed of welding point is slow, which makes the needle-shaped martensite become coarse. Under low electrode pressure of 0.15 MPa, the surface of resistance spot welding plate is rugged. The upper and the lower plates are not tightly connected, and the defects, such as porosity and kissing bond, are easy to be produced during welding, as shown in Figs.5(a, b). When the electrode pressure is 0.20 MPa (Figs.5(c, d)), the flawless resistance spot welding joints can be obtained, which greatly improves the mechanical properties of the solder joints. When the electrode pressure is too high, the upper and the lower plates are closely connected. The residual oxide, oil and

other impurities on the surface of the plate are difficult to be discharged by the gas generated by the high temperature metallurgical reaction, resulting in the formation of welding pores, as shown in Figs.5(e, f).

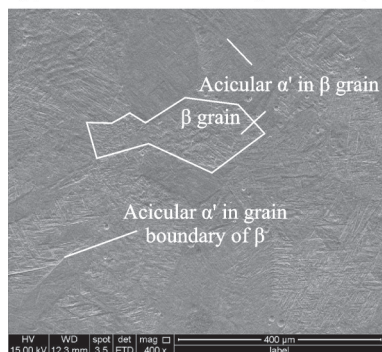
Fig.6 shows the microhardness curves of the



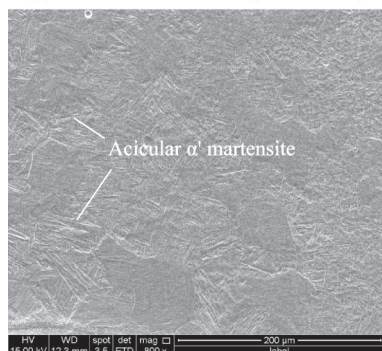
(a) Microstructure of NZ ( $p=0.15$  MPa)



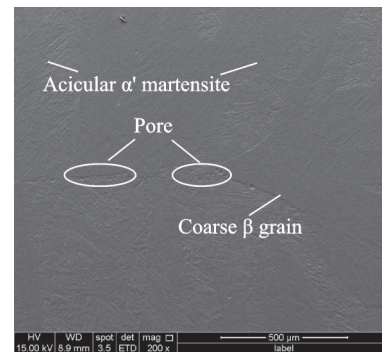
(b) Microstructure of HAZ ( $p=0.15$  MPa)



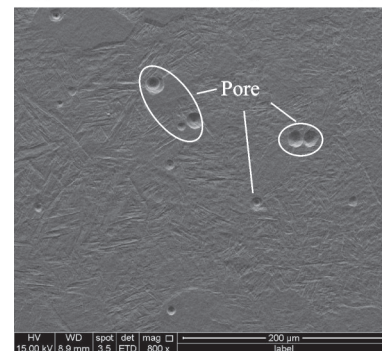
(c) Microstructure of NZ ( $p=0.20$  MPa)



(d) Microstructure of HAZ ( $p=0.20$  MPa)



(e) Microstructure of NZ ( $p=0.25$  MPa)



(f) Microstructure of HAZ ( $p=0.25$  MPa)

Fig.5 Microstructures of resistance spot welding joints in different regions

white dotted resistance spot welding joints which are showed in Fig.4. It can be seen from the figure that the microhardness of nugget zone is generally higher than that of HAZ. The main reason is that the temperature of NZ is high and the cooling rate is fast, and a large amount of acicular  $\alpha'$  martensite is produced in the cooling process after welding. It improves the mechanical properties of NZ. The microhardness of HAZ is the lowest in the whole solder joints, which is the weak area of solder joints. When the electrode pressure is 0.15 MPa, the microhardness in the central region of nugget decreases to the lowest, which is due to a large number of welding defects in this region. When the electrode pressure is too high, i.e. 0.25 MPa, owing to the serious heat accumulation in NZ, the grain size is abnormally coarse and the microhardness of NZ decreases correspondingly. However, when  $p=0.20$  MPa, there is a few defects in the joint, and the grain size in NZ is smaller, so it has higher microhardness.

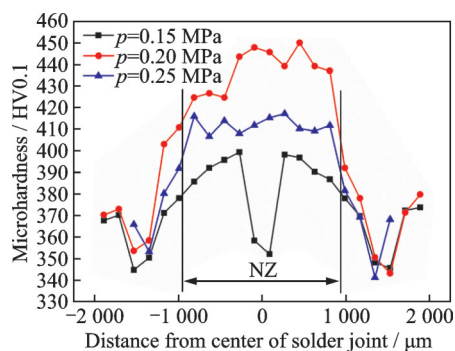
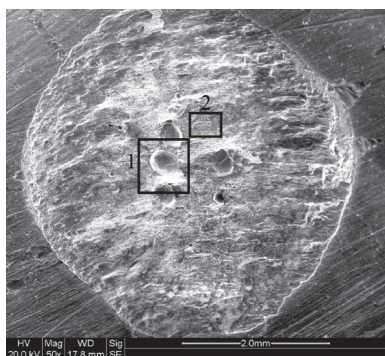


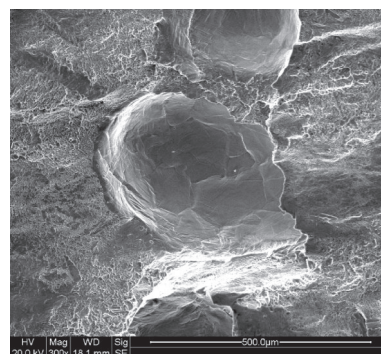
Fig.6 Microhardness distribution of resistance spot welding joints

### 2.3 Fracture morphology

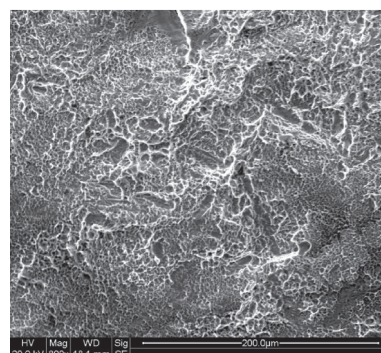
Fig.7 shows the fracture morphology of solder joints under the optimal process parameters: Welding time of 10 ms, electrode pressure of 0.20 MPa and welding current of 46 A. It can be seen from Fig.7(a) that the fracture surface of resistance spot weld presents a typical button fracture, and the crack initiates in the weakest area of the solder joints, that is, HAZ, and it propagates to NZ. By enlarging different typical fracture regions, it can be found that Region 1 (Fig.7(b)) presents typical intergranular fracture mode, forming large tearing holes. Tearing edges are distributed around the holes, and there are typical cleavage surfaces inside the holes, which are mainly caused by the coarse  $\beta$ -columnar crystals in NZ; a large number of small dimples can be clearly seen in Region 2 (Fig.7(c)), and there are ductile faults in this area. Therefore, the fracture mode of spot weld is intergranular brittle-ductile fracture.



(a) Macro fracture of solder joints



(b) Fracture morphology of Region 1



(c) Fracture morphology of Region 2

Fig.7 Fracture morphology of solder joints

## 3 Conclusions

The detailed conclusions were drawn from this research as follows.

(1) 2 mm Ti-4Al-1.5Mn plate was successfully welded by resistance spot welding. When the electrode pressure is 0.20 MPa and the welding current is 46 A, the maximum shear load of 8.80 kN.

(2) The nugget zone is mainly composed of coarse  $\beta$ -columnar grains, which is a typical as-cast structure. The phase composition is mainly composed of coarse acicular martensite, which is arranged in a certain orientation. The fracture mode of resistance spot weld is intergranular brittle-ductile fracture.

### References

- [1] SHOKATI A A, ZHOU Y, WEN Z, et al. Dissimilar joining of carbon/carbon composites to Ti6Al4V using reactive resistance spot welding[J]. Journal of Alloys and Compounds, 2019, 772: 418-428.
- [2] ADAMUS J. Applications of titanium sheets in modern building construction[J]. Advanced Materials Research, 2014, 1020: 9-14.

- [3] CUI C, HU B, ZHAO L, et al. Titanium alloy production technology, market prospects and industry development[J]. *Materials and Design*, 2011, 32: 84-91.
- [4] BREWER W D, BIRD K R, WALLACE T A, et al. Titanium alloys and processing for high-speed aircraft[J]. *Materials Science & Engineering: A*, 1998, 243: 299-304.
- [5] TAO Jie, HUANG Zhendong, LIU Hongbing, et al. Preparation and characterization of anti-oxidation enamel coating for Ti-based alloys at high temperature[J]. *Journal of Nanjing University of Aeronautics & Astronautics*, 2010, 42(4): 505-509. (in Chinese)
- [6] CHEN Y, DING L Y, FU Y C, et al. Dry grinding of titanium alloy using brazed monolayer CBN wheels coated with graphite lubricant[J]. *Transactions of Nanjing University of Aeronautics & Astronautics*, 2014, 31(1): 1-15.
- [7] WANG Z, SHEN J, HU S, et al. Investigation of welding crack in laser welding brazing welded TC4/6061 and TC4/2024 dissimilar butt joints[J]. *Journal of Manufacturing Processes*, 2020, 60: 54-60.
- [8] LI S, CHEN Y, KANG J, et al. Interfacial microstructures and mechanical properties of dissimilar titanium alloy and steel friction stir butt-welds[J]. *Journal of Manufacturing Processes*, 2019, 40: 160-168.
- [9] GHOSH M, CHATTERJEE S. Effect of interface microstructure on the bond strength of the diffusion welded joints between titanium and stainless steel[J]. *Materials Characterization*, 2005, 54(4/5): 327-337.
- [10] ZHENG Y, ZHAO Z, ZHANG Z, et al. Internal crack initiation characteristics and early growth behaviors for very-high-cycle fatigue of a titanium alloy electron beam welded joints[J]. *Materials Science & Engineering: A*, 2017, 706: 311-318.
- [11] LIN J Y, SHOICHI N, TOSHIHIKO K, et al. Interfacial phenomena during ultrasonic welding of ultra-low-carbon steel and pure Ti[J]. *Scripta Materialia*, 2020, 178: 218-222.
- [12] KAHRAMAN N. The influence of welding parameters on the joint strength of resistance spot-welded titanium sheets[J]. *Materials and Design*, 2007, 28(2): 420-427.
- [13] ZHANG H, WANG F, XI T, et al. A novel quality evaluation method for resistance spot welding based on the electrode displacement signal and the Chernoff faces technique[J]. *Mechanical System and Signal Processes*, 2015, 62/63: 31-43.
- [14] WAN X, WANG Y, ZHANG P, et al. Modelling the effect of welding current on resistance spot welding of DP600 steel[J]. *Journal of Materials Processing Technology*, 2014, 214: 3-9.
- [15] CHEN F, TONG G Q, MA Z W, et al. The effects of welding parameters on the small scale resistance spot weldability of Ti-1Al-1Mn thin foils[J]. *Materials and Design*, 2016, 102: 174-185.
- [16] CHEN S, SUN T, JIANG X, et al. Online monitoring and evaluation of the weld quality of resistance spot welded titanium alloy[J]. *Journal of Manufacturing Processes*, 2016, 23: 183-191.
- [17] WEI P, WU T. Workpiece property effects on nugget microstructure determined by heat transfer and solidification rate during resistance spot welding[J]. *International Journal of Thermal Science*, 2014, 86: 1-9.
- [18] WEI P, WU T. Electrode geometry effects on microstructure determined by heat transfer and solidification rate during resistance spot welding[J]. *International Journal of Heat and Mass Transfer*, 2014, 79: 8-16.
- [19] POURANVARI M, MARASHI S. Critical review of automotive steels spot welding: process, structure and properties[J]. *Science and Technology of Welding and Joining*, 2013, 18: 361-403.
- [20] HAYAT F. Effect of aging treatment on the microstructure and mechanical properties of the similar and dissimilar 6061-T6/7075-T651 RSW joints[J]. *Materials Science & Engineering: A*, 2012, 556: 34-43.
- [21] SPENA P R, MADDIS M, LOMBARDI F, et al. Mechanical strength and fracture of resistance spot welded advanced high strength steels[J]. *Procedia Engineering*, 2015, 109: 50-64.
- [22] FENG Y, ZENG K, HE X, et al. Fatigue property analysis of TA1 pure titanium resistance spot welding joint[J]. *Nonferrous Metals Engineering*, 2018, 8(1): 7-12.
- [23] JIANG L, LIN L, JIANG H, et al. Analysis of microstructure and properties of pure titanium/magnesium alloy dissimilar material resistance spot welding joint[J]. *Welding*, 2018, 7: 39-42.

**Acknowledgements** This work was supported by the Priority Academic Program Development of Jiangsu Higher Education Institution and Beijing Institute of Aeronautical Materials (No.KZ82171509).

**Authors** Mr. JIANG Jian received the B. S. degree in College of Materials Science and Technology of Nanjing University of Aeronautics and Astronautics in June 2017. He

joined in College of Materials Science and Technology of Nanjing University of Aeronautics and Astronautics in September 2017, where he is a Ph.D. candidate. His major is materials processing engineering and his research focuses on the welding of titanium alloy.

Prof. SHEN Yifu received the B. S. degree in Chongqing University, Chongqing, China, in 1988. He received the M. S. and Ph.D. degrees in Institute of Metals, Chinese Academy of Sciences, in 1993 and 1998, respectively. From 1999 to 2003, he was a postdoctoral researcher at Nanjing University of Aeronautics and Astronautics. From 1993 to present, he has been with College Materials Science and Technolo-

gy, Nanjing University of Aeronautics and Astronautics. His research has focused on friction stir welding and processing, laser rapid forming and metal surface engineering.

**Author contributions** Prof. SHEN Yifu designed the study. Mr. JIANG Jian performed the experiments and wrote the paper. Mr. ZHANG Mingjie reviewed the manuscript. Ms. QI Lichun contributed to background of the study. Mr. CHEN Wenhua manufactured the samples. All authors commented on the manuscript draft and approved the submission.

**Competing interests** The authors declare no competing interests.

(Production Editor: XU Chengting)

## Ti-4Al-1.5Mn 电阻点焊接头的组织与力学性能

江 剑<sup>1</sup>, 齐立春<sup>2</sup>, 张明杰<sup>2</sup>, 陈文华<sup>1</sup>, 沈以赴<sup>1</sup>

(1. 南京航空航天大学材料科学与技术学院, 南京 211106, 中国;

2. 北京航空材料研究院钛合金研究所, 北京 100095, 中国)

**摘要:**采用气动电阻点焊机对Ti-4Al-1.5Mn双相钛合金薄板进行了点焊。研究了不同焊接工艺参数对剪切载荷和熔核直径的影响。结果表明,焊点的最大剪切载荷随电极压力和焊接电流的增大先增大后减小,而熔核直径随电极压力和焊接电流的增大而增大。最佳工艺参数为电极压力0.20 MPa,焊接电流46 A,焊点最大剪切载荷为8.80 kN。熔核区组织为粗针状马氏体,焊点以晶间脆-韧性断裂的混合方式失效。

**关键词:**钛合金;电阻点焊;剪切载荷;显微组织